PNAS RESEARCH ARTICLE | MEDICAL SCIENCES

Sfrp4 is required to maintain Ctsk-lineage periosteal stem cell niche function

Ruiying Chen[a,1], Han Dong[b], Dhairya Raval[a], David Maridas[c], Sudipta Baroi[a], Kun Chen[a], Dorothy Hu[a], Shawn R. Berry[a], Roland Baron[a,d], Matthew B. Greenblatt[e,f], and Francesca Gori[a,2]

Edited by Karen M. Lyons, University of California, Los Angeles, CA; received July 28, 2023; accepted October 6, 2023 by Editorial Board Member Brigid L. Hogan

We have previously reported that the cortical bone thinning seen in mice lacking the Wnt signaling antagonist *Sfrp4* is due in part to impaired periosteal apposition. The periosteum contains cells which function as a reservoir of stem cells and contribute to cortical bone expansion, homeostasis, and repair. However, the local or paracrine factors that govern stem cells within the periosteal niche remain elusive. Cathepsin K (Ctsk), together with additional stem cell surface markers, marks a subset of periosteal stem cells (PSCs) which possess self-renewal ability and inducible multipotency. *Sfrp4* is expressed in periosteal Ctsk-lineage cells, and *Sfrp4* global deletion decreases the pool of PSCs, impairs their clonal multipotency for differentiation into osteoblasts and chondrocytes and formation of bone organoids. Bulk RNA sequencing analysis of Ctsk-lineage PSCs demonstrated that *Sfrp4* deletion down-regulates signaling pathways associated with skeletal development, positive regulation of bone mineralization, and wound healing. Supporting these findings, *Sfrp4* deletion hampers the periosteal response to bone injury and impairs Ctsk-lineage periosteal cell recruitment. Ctsk-lineage PSCs express the PTH receptor and PTH treatment increases the % of PSCs, a response not seen in the absence of *Sfrp4*. Importantly, in the absence of *Sfrp4*, PTH-dependent increase in cortical thickness and periosteal bone formation is markedly impaired. Thus, this study provides insights into the regulation of a specific population of periosteal cells by a secreted local factor, and shows a central role for Sfrp4 in the regulation of Ctsk-lineage periosteal stem cell differentiation and function.

Cathepsin K-lineage periosteal stem cells | periosteum | Sfrp4 | PTH | bone repair

Significance

The periosteum is a major source of stem cells that contribute to cortical expansion during growth, cortical homeostasis in the adult skeleton, bone repair, and to the response to anabolic drugs. Local factors influencing the periosteal stem cell niche are still poorly understood. Here, we focus on a recently identified population of periosteal Ctsk-lineage stem cells and report the role of *Sfrp4* in their function and response to anabolic drugs. The identification of signaling molecules regulating periosteal stem cell populations provides an outstanding opportunity to advance our understanding of the mechanisms governing periosteal stem cells and may help identifying specific therapeutic options for human diseases associated with bone fragility and impaired bone healing and bone regeneration.

Secreted Frizzled Receptor Protein (Sfrp) 1 to 5 (in mammals) are secreted Wnt inhibitors essential for the development and homeostasis of several tissues and organs, including bone (1–6). Sfrps have an N-terminal cysteine-rich domain (CRD), which share 30 to 50% homology with the CRD domain of the frizzled receptors, and a C-terminal netrin (NTR)-like domain (1, 2, 5, 6). Sfrps function as Wnt decoy receptors that can either bind Wnt ligands and prevent binding to their receptor/coreceptor complexes or form a nonfunctional complex with the CRD motif of the Frizzled receptors (2, 7). We were the first to report that loss of function mutations of the Wnt inhibitor Secreted Frizzled Receptor Protein 4 (*SFRP4*) lead to Pyle disease (*OMIM-265900*), a rare skeletal disorder with limb deformity characterized by wide metaphysis and cortical thinning and increased fragility fractures (8). Additionally, individuals with Pyle disease present with skull anomalies, characterized by increased diploe and thinner calvarial bone (8). The association between mutations in SFRP4 and Pyle diseases has been sequentially confirmed (9–11). *Sfrp4* deletion in mice causes limb and calvarial deformities closely mimicking those seen in individuals with Pyle disease (8, 12, 13). Using *Sfrp4*$^{-/-}$ mice, we uncovered that in the long bones, Sfrp4 contributes to cortical bone homeostasis by regulating periosteal bone formation and endosteal remodeling (8, 14). We have shown that Sfrp4 regulation of the endosteal remodeling occurs mainly via local repression of noncanonical Wnt signaling (14); however, the exact mechanism(s) by which *Sfrp4* deletion decreased periosteal bone formation is unknown.

The periosteum, which lines the external surface of cortical bone, contains a niche housing a distinct set of stem cells, osteoprogenitors, and osteoblasts that contribute to cortical expansion during growth, to cortical homeostasis in the adult skeleton, to the response to anabolic drugs, such as parathyroid hormone (PTH), and to injury repair (13, 15–24). Using lineage tracing methods, to trace Prx1^{+}, aSma^{+}, Gli1^{+}, Sox9^{+}, Col2^{+}, and Lepr^{+} cells among others, recent studies have identified lineage-restricted periosteal embryonic and adult periosteal cells with multipotent differentiation ability and with an important role during cortical bone growth and repair, (15, 17–19, 25–30). While studies

Author contributions: R.C., R.B., M.B.G., and F.G. designed research; R.C., H.D., D.R., D.M., S.B., K.C., and F.G. performed research; R.C., H.D., D.R., D.M., S.B., K.C., and F.G. analyzed data; D.H. and S.R.B. performed histomorphometry and microCT measurements, respectively; R.B. and M.B.G. edited the manuscript; and R.C. and F.G. wrote the paper.

The authors declare no competing interest.

This article is a PNAS Direct Submission. K.M.L. is a guest editor invited by the Editorial Board.

[1]Present address: Department of Oral Implantology, Shanghai Ninth People's Hospital, Shanghai Jiao Tong University School of Medicine, College of Stomatology, National Center for Stomatology, National Clinical Research Center for Oral Diseases and Shanghai Key Laboratory of Stomatology, Shanghai 200023, China.

[2]To whom correspondence may be addressed. Email: Francesca_gori@hsdm.harvard.edu.

This article contains supporting information online at https://www.pnas.org/lookup/suppl/doi:10.1073/pnas.2312677120/-/DCSupplemental.

Published November 6, 2023.

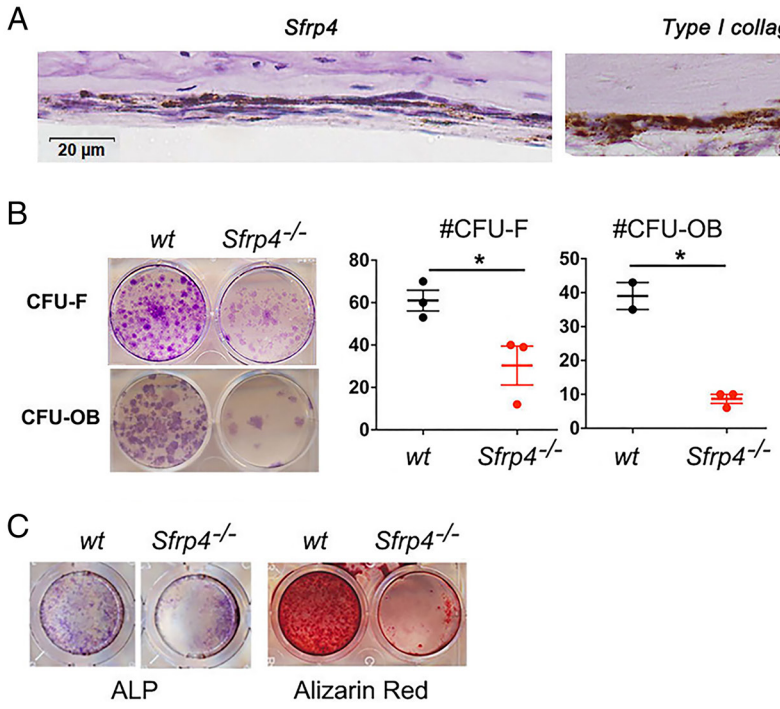

Fig. 1. *Sfrp4* deletion impairs periosteal cell clonal potential and differentiation. (*A*) Representative images of *Sfrp4* and *Type I Collagen* expression in the long bone periosteum of *wt* mice detected by RNAscope (n = 3). (Scale bar, 20 µm.) (*B*) Representative images of CFU-F and CFU-OB assay and quantification of periosteal cells isolated from 4-wk-old *wt* and *Sfrp4*$^{-/-}$ mice. (*C*) Representative images of ALP and Alizarin Red staining of periosteal cells isolated from *wt* and *Sfrp4*$^{-/-}$ mice. (n = 3, each point = 1 mouse). All data are expressed as mean ± SEM. **P* < 0.05 and *****P* < 0.0001 by an unpaired Student *t* test.

to identify and characterize the periosteal stem cell niche are on the rise, our understanding of the paracrine and local factors involved in establishing and maintaining them as well as in influencing their behavior is still evolving. Investigations into these regulatory factors might be of considerable help to identify specific drug targets that can increase periosteal bone formation. This would be important for the treatment of skeletal diseases, such as Pyle disease where cortical thickness is markedly impaired or severe osteoporosis where cortical fragility is present. To further understand the cortical phenotype seen in Pyle disease, we asked the question of whether Sfrp4 might regulate cortical bone homeostasis by influencing periosteal stem cells. Here, we focused on a subset of recently identified periosteal cells labeled by Cathepsin K (Ctsk). Although Ctsk is known as a pivotal lysosomal cysteine

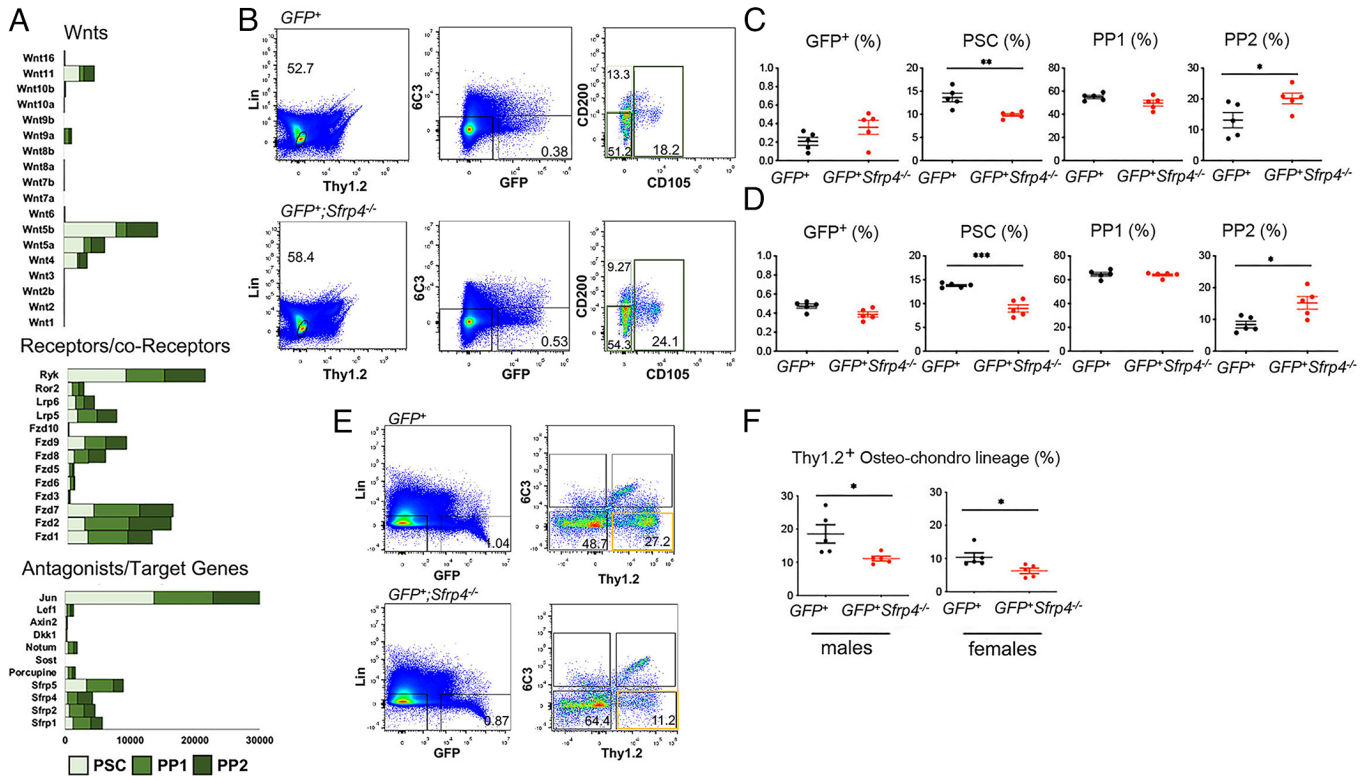

Fig. 2. *Sfrp4* deletion affects the % of Ctsk-lineage periosteal cell population. (*A*) Bulk RNAseq. Expression levels of Wnt signaling pathway components (GSE106235). (*B*) Gating details of flow cytometry. (*C* and *D*) Percentage of PSCs, PP1, and PP2 cells in 4-wk-old *GFP*$^{+}$ *and GFP*$^{+}$*Sfrp4*$^{-/-}$ male (*C*) and female (*D*) mice. (*E*) Gating details of flow cytometry. (*F*) Percentage of Thy1.2^{+} osteo-chondro progenitors in 4-wk-old *GFP*$^{+}$ *and Ctsk GFP*$^{+}$*Sfrp4*$^{-/-}$ male and female. (n = 5 each point = 2 mice). All data: mean ± SEM, **P* < 0.05 and ***P* < 0.01 by the Student *t* test.

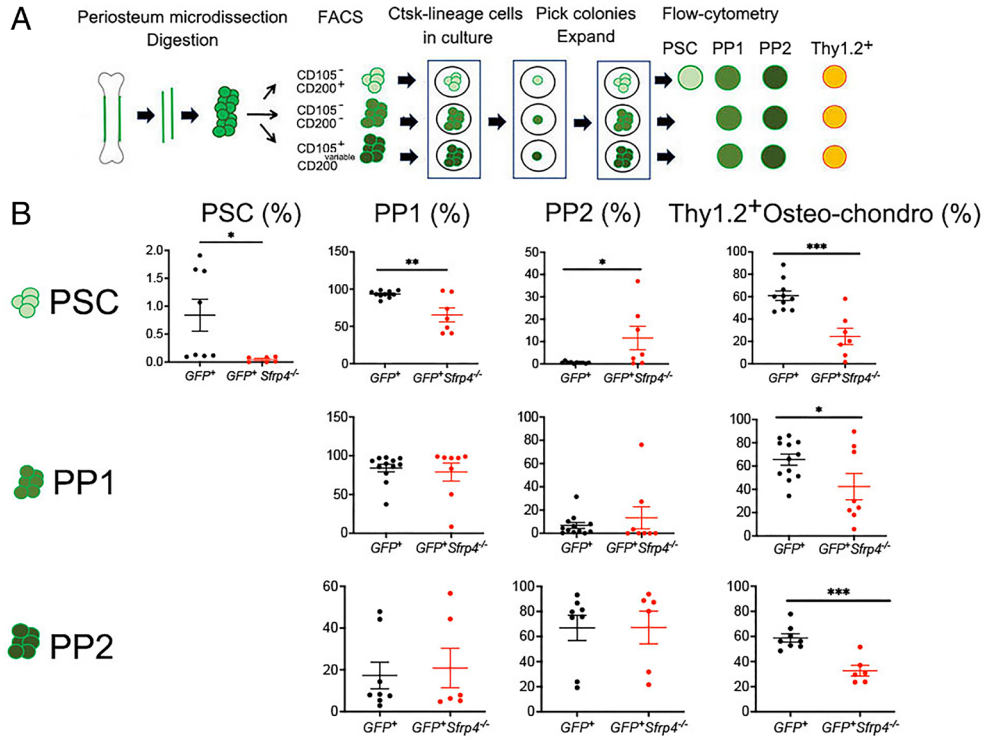

Fig. 3. *Sfrp4* deletion impairs Ctsk-lineage cell stemness and cell lineage restriction. (*A*) Schematic diagram of Ctsk-lineage PSC, PP1, and PP2 cells in-vitro expansion and resorting method. (*B*) Percentage of PSC, PP1, and PP2 cells and Thy1.2^{+} osteo/chondro-lineage cells in single PSC, PP1, and PP2 cell colony after 7-d expansion from *GFP and GFP^{+}Sfrp4$^{-/-}$* mice. (n = 7 to 9) All data: mean ± SEM, $^{*}P<0.05$ and $^{**}P<0.01$ $^{***}P<0.005$ by the Student *t* test.

protease involved in bone resorption (31–33), Debnath et al., using Ctsk-Cre (*CtskCre*) mice with the *mTmG* reporter mouse, have found that in addition to the expected ability to label osteoclasts, CtskCre labels also a pool of periosteal mesenchymal cells (Ctsk^{+}GFP^{+}) but not endosteal mesenchyme (17). Using skeletal stem cell/progenitor surface markers (34–36), they demonstrated that Ctsk-lineage periosteal cells comprise three distinct periosteal mesenchymal subpopulations, all Lin^{-}Thy1.2^{-}6C3^{-} GFP^{+}:1) bona fide periosteal stem cells (PSCs) (CD105^{-}CD200^{+}), 2) non-stem periosteal progenitors 1 (PP1) (CD105^{-}CD200^{-}), and 3) non-stem periosteal progenitors 2 (PP2) (CD105^{+}CD200^{variable}) (17). Ctsk-lineage PSCs form bone via intramembranous ossification and contribute to fracture repair via endochondral bone formation. Hence, the exact nature of local factors and signaling cues regulating these periosteal cells remains to be determined.

We searched the bulk RNA-Seq database generated by Debnath et al. (GSE106235) (17) for the expression of members of the Wnt signaling cascade in the distinct pools of periosteal stem cells/progenitors. Not surprisingly, Ctsk-lineage PSCs, PP1, and PP2 cells all express several components of the Wnt signaling machinery, although at different levels. Interestingly, we noted that Wnt components classically associated with noncanonical Wnt cascades were generally strongly expressed in these cells. Most importantly, we found that *Sfrp4* is expressed in periosteal Ctsk-lineage cells, prevalently in PP1 and PP2 cells suggesting, together with our findings of impaired periosteal formation in the absence of *Sfrp4* (8), a potential role for Sfrp4 within these periosteal cell population.

To gain insight into the function of Sfrp4 in the regulation of the Ctsk-lineage periosteal stem/progenitor cell differentiation and function, we generated *CtskCre;mTmG;wt* (*GFP^{+}*) and *CtskCre;mTmG;Sfrp4$^{-/-}$* (*GFP^{+};Sfrp4$^{-/-}$*) mice and investigated Ctsk^{+} (GFP^{+}) labeled and GFP^{+};Sfrp4$^{-/-}$ periosteal cells. Our studies show a secreted factor, Sfrp4, with a function in a specific lineage of periosteal stem cells. Collectively, our data highlight the previously unknown role of Sfrp4 in the regulation of periosteal stem/progenitor cell lineage commitment, physiological function, and response to anabolic drugs, providing an opportunity to advance our understanding of the periosteum and potentially to specific therapeutic options for human diseases associated with cortical bone fragility.

Results

***Sfrp4* Is Expressed in the Periosteum, and Its Deletion Impairs Periosteal Cell Osteogenic Differentiation.** We first examined *Sfrp4* expression in the long bone periosteum. As shown in Fig. 1*A*, *Sfrp4* was detected in the inner periosteal cell layer adjacent to bone, which also expresses *Type I Collagen,* and it is known to host stem cells. To evaluate the role of *Sfrp4* in the periosteum, periosteal cells were isolated from the whole periosteum of *wt* and *Sfrp4$^{-/-}$* mice and their ability to form CFU-F and CFU-OB assessed. As shown in Fig. 1*B*, *Sfrp4*-deficient cells display a significant decrease in the number of CFU-F and CFU-OB colonies. Additionally, *Sfrp4*-deficient periosteal cells displayed a decrease in osteogenic differentiation as shown by a decrease in ALP and Alizarin Red staining (Fig. 1*C*). Confirming our previous findings of impaired periosteal formation in *Sfrp4$^{-/-}$* mice (8), bone histomorphometry analysis shows that at 4 wk of age, *Sfrp4* deletion leads to a significant decrease in periosteal mineralized surface (Ps. MS/BS), mineral apposition rate (Ps.MAR), bone formation rate (Ps.BFR/BS), and cortical thickness (*SI Appendix*, Fig. S1).

***Sfrp4* Deletion Affects the Distribution of Ctsk-Lineage Periosteal Cells.** Cells expressing Ctsk in the periosteum identify a population of stem cells and non-stem progenitors (17). Because of our focus on Sfrp4 and Wnt signaling, we searched the bulk RNA-Seq database previously generated (17) for the expression of members of the Wnt signaling cascade in the distinct pools of Ctsk-lineage periosteal cells. Ctsk-lineage PSCs, PP1, and PP2 cells express several components of the Wnt signaling machinery, although at different levels (Fig. 2*A*) (17). Interestingly, we noted that Wnt components classically associated with noncanonical Wnt cascades, such as *Wnt4*, *Wnt5a*, *Wnt5b*, *Wnt11*, *c-jun*, and *Ryk*, were generally strongly expressed in these cells, while canonical ligands such as *Wnt1* and

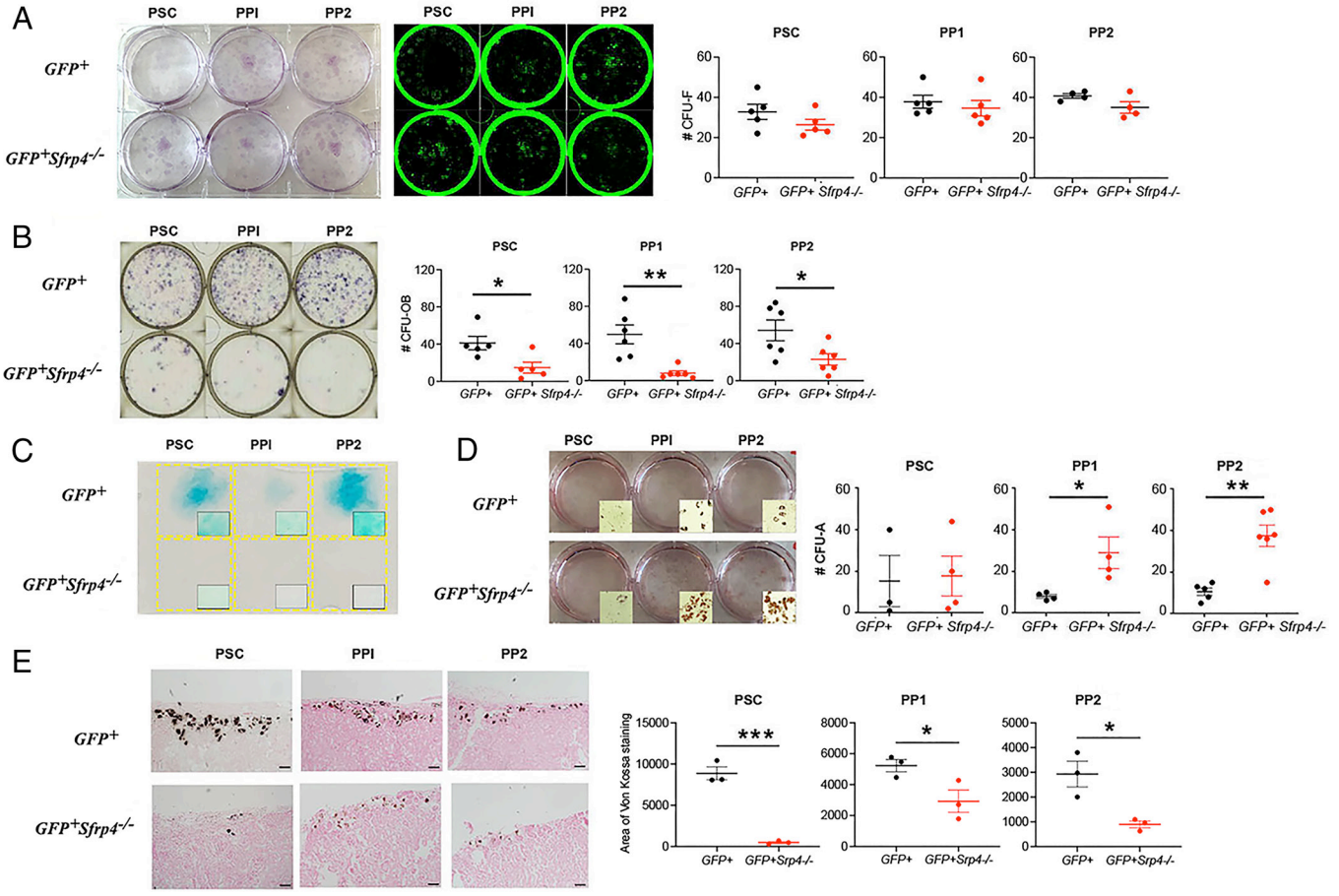

Fig. 4. *Sfrp4* deletion impairs Ctsk-lineage periosteal cell function. (*A–D*) Representative images and quantification of CFU-F (*A*), CFU-OB (*B*), CFU-Chondro (*C*), and CFU-Adipo (*D*) assays from PSC, PP1, and PP2 cells. All data are expressed as mean ± SEM. *$P < 0.05$ and **$P < 0.01$ by the Student *t* test (n = 4 to 8, 1 point = 2 mice). (*E*) Representative images and quantification of the Von Kossa staining area for the in vivo kidney transplantation assay. (Scale bar, 100 μm.) All data are expressed as mean ± SEM. *$P < 0.05$ and ***$P < 0.001$ by the Student *t* test.

Wnt3a or downstream target genes such as *Axin2*, *Dkk1,* and *Lef1* were not (Fig. 2*A*). Most importantly, *Sfrp4* is expressed in all Ctsk-lineage periosteal cell populations and predominantly expressed in PP1 and PP2 cells (Fig. 2*A*). These findings support a potential crosstalk between Sfrp4 and noncanonical Wnt signaling which we have shown to be involved in the cortical phenotype seen in *Sfrp4* null mice (8, 14). We therefore generated *Ctskcre;mTmG;WT* (*GFP*$^+$) and *Ctskcre;mTmG;Sfrp4*$^{-/-}$ (*GFP*$^+$*Sfrp4*$^{-/-}$) mice and isolated PSCs, PP1, and PP2 cells from the long bones of *GFP*$^+$ (*Ctsk*$^+$) *and GFP*$^+$*Sfrp4*$^{-/-}$mice using multicolor flow cytometry and a panel of cell surface markers previously used (17). Flow cytometry analysis showed that *Sfrp4* global deletion leads to a significant decrease in the relative % of PSCs, while markedly increasing the relative % of PP2 cells in both male and female mice (Fig. 2 *B–D*). A similar phenotype was also seen in Ctsk-lineage PSCs, PP1, and PP2 cells isolated from calvaria of *GFP*$^+$ (*Ctsk*$^+$) *and GFP*$^+$*Sfrp4*$^{-/-}$mice (*SI Appendix*, Fig. S2). Importantly, we found that the % of Lin$^-$Thy1.2$^+$C63$^-$ GFP$^+$ defined as Thy1.2$^+$osteo-chondro progenitor cells (34) was significantly decreased in the periosteum isolated from *GFP*$^+$*Sfrp4*$^{-/-}$ mice (Fig. 2 *E* and *F*). Thus, altogether, these studies suggested that *Sfrp4* global deletion decreased the pool of Ctsk-lineage PSCs and favored their transition into PP2 progenitors, while blocking their progression into Thy1.2$^+$osteo-chondro progenitors.

Sfrp4 Influences the Pool of Ctsk-Lineage PSCs and Their Differentiation. Ctsk-lineage PSCs sit at the apex of a differentiation hierarchy and give rise to themselves (self-renewal) and to their progeny, PP1 and PP2 cells (17). To test whether *Sfrp4* deletion influences Ctsk-lineage differentiation hierarchy, we carried out a round of sequential cell fractionation based on cell surface markers and flow cytometry in which PSCs, PP1, and PP2 cells were sorted from *GFP*$^+$ and *GFP*$^+$*Sfrp4*$^{-/-}$ mice, plated and cultured. After 7 d in culture, at least 10 single colonies were isolated from PSC, PP1, or PP2 cell culture, recultured for another 7 d, and reanalyzed by flow cytometry (Fig. 3*A*). *Sfrp4* deletion significantly impaired the ability of PSCs to give rise to PSCs and PP1 cells while favoring their progression into PP2 non-stem progenitors (Fig. 3*B*). Confirming our previous data (Fig. 2), *Sfrp4* deleted PSCs present with impaired ability to give rise to Thy1.2$^+$ osteo-chondroprogenitors (Fig. 3*B*). Confirming previous findings and demonstrating that in vitro assays can be used to generate differentiation hierarchies that parallel in vivo organoid-based assays, PP1 and PP2 cell populations, did not give rise to PSC (17) (Fig. 3*B*). While *Sfrp4* deletion did not impair PP1 and PP2 cell ability to give rise to themselves, it impaired their ability to differentiate into Thy1.2$^+$ osteo-chondroprogenitors (Fig. 3*B*). These data suggest that while Sfrp4 deletion depletes the PSC pool and favors their transition to non-stem progenitors, it significantly impairs their transition to the Thy1.2$^+$ osteo-chondro lineage. In addition, given that these studies were carried out with Ctsk-lineage sorted cells, our findings suggest cell-autonomous effects of Sfrp4 on the composition of the pool of Ctsk-lineage periosteal cells.

***Sfrp4* Deletion Alters Ctsk-Lineage PSC, PP1, and PP2 Cell Multipotency.** We next explored whether Sfrp4 deletion impaired in vitro clonal differentiation capacity of Ctsk-lineage periosteal cells. While no significant differences were seen in the ability of

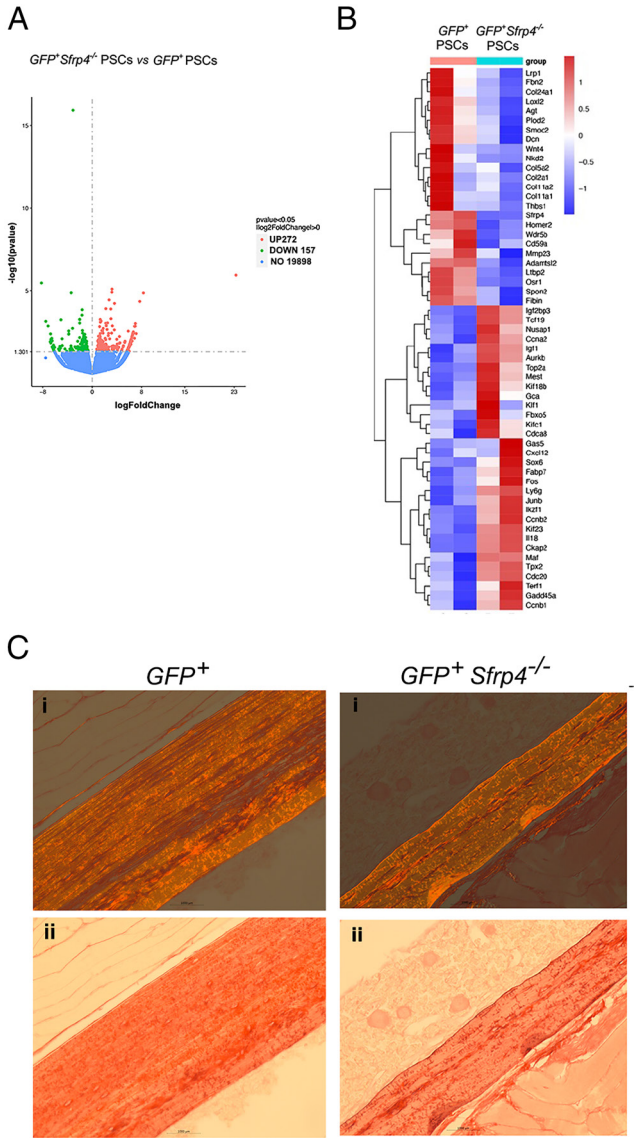

Fig. 5. Differentially expressed genes in the PSC cell population. (*A*) Volcan plot. (*B*) Heatmap showing the first 25 down-regulated and up-regulated genes. (*C*) Representative images of cortical bone stained with Picro Sirius red i = fluorescence and ii = brightfield. (Scale bar, 1,000 µm.) (n = 3).

Sfrp4-deficient cells to form CFU-F, the number of CFU-OB colonies formed by *GFP*$^+$*Sfrp4*$^{-/-}$ PSCs, PP1, and PP2 cells was significantly lower compared to those formed by their *GFP*$^+$ counterparts (Fig. 4 *A* and *B*). In vitro chondrogenic differentiation of *GFP*$^+$*Sfrp4*$^{-/-}$ PSCs, PP1, and PP2 cells was also markedly decreased compared to that of *GFP*$^+$ PSCs, PP1, and PP2 cells (Fig. 4*C*). Conversely in vitro adipogenic colony formation was significantly increased in all *GFP*$^+$*Sfrp4*$^{-/-}$ periosteal cell populations (Fig. 4*D*). Overall, these data confirmed that *Sfrp4* deletion impairs the differentiation of Ctsk-lineage periosteal cells into the chondro- and osteoblast lineages and suggest that Sfrp4 might regulate the lineage allocation of Ctsk-lineage PSC and progenitor cells.

Previous studies have shown that Ctsk-lineage periosteal cells in bone organoids mediate intramembranous ossification (17). We therefore assessed the ability of Ctsk-lineage PSCs and non-stem progenitors to form bone organoids in vivo. As shown in Fig. 4*E*, Von Kossa staining showed a significant decrease of mineralized bone after transplantation of *GFP*$^+$*Sfrp4*$^{-/-}$ PSCs compared to the *GFP*$^+$PSCs transplanted group under the kidney capsule of *wt* mice. Similar results were observed when *GFP*$^+$*Sfrp4*$^{-/-}$ PP1 and PP2 cells were transplanted into the renal capsule of *wt* mice. Overall, these data support a cell-autonomous role for Sfrp4 in the overall differentiation of Ctsk-lineage periosteal cells.

***Sfrp4* Deletion Impairs Signaling Pathways Associated with Bone Regeneration, Wound Healing, and Mineralization in Ctsk-Lineage PSCs.** To better understand the changes occurring in the Ctsk-lineage PSC population in the absence of *Sfrp4*, we performed bulk RNA-seq analysis (GSE236686) (37). Two biological samples were collected per *GFP*$^+$ PSC and *GFP*$^+$*Sfrp4*$^{-/-}$ PSCs, each composed of the pooled cells yield from n = 3 mice. We identified 429 differentially expressed genes, of which 272 were up-regulated and 157 were down-regulated in *GFP*$^+$*Sfrp4*$^{-/-}$ PSCs (Fig. 5*A* and *SI Appendix*, Fig. S3). Among the genes significantly down-regulated in *GFP*$^+$*Sfrp4*$^{-/-}$ PSCs, we found several collagens (Col2a1, Col11a1, Col11a2, and Col5a2), ECM proteins with a known role in collagen cross-linking and supporting osteoblast differentiation, including Loxl2, SPARC-related modular calcium-binding protein1 (SMOC1), thrombospondin1, and decorin, and components of Wnt signaling such as Wnt4, Lrp1, and Nkd2 (Fig. 5*B*). The orphan nuclear receptors coding gene NR4A2 (Nurr1), known to be induced by PTH and to have a role in bone metabolism by regulating the expression of several osteoblastic marker genes including Bglap and Col1a among others (38–40), was also found to be decreased by *Sfrp4* deletion. Gene ontology (GO) and reactome analysis reveal that pathways related to skeletal system development, extracellular matrix organization, wound healing, and positive regulation of bone mineralization were down-regulated in *GFP*$^+$*Sfrp4*$^{-/-}$ PSCs (Tables 1 and 2). Because several collagen genes were altered, we performed Sirius red staining to explore collagen fibrils organization and as shown in Fig. 5*C*, lack of *Sfrp4* leads to a disorganization of collagen fibrils in cortical bone.

Among the up-regulated genes, we found several cell-cycle regulators, including Ccna2, Ccnb1, Ccnb2, Cdca8, and Cdc20 (Fig. 5*B*). Accordingly, GO and reactome analysis reveals that pathways related to regulation of cell cycle machinery were up-regulated, suggesting a potential switch from stem cell maintenance to lineage determination (Tables 1 and 2). However, the proliferation of PSC, PP1, or PP2 populations, measured after EdU injection and FACS analysis, showed only a trend toward an increase in the percentage of Edu$^+$ PSCs and PP1 cells from *GFP*$^+$*Sfrp4*$^{-/-}$ mice (*SI Appendix*, Fig. S3).

***Sfrp4* Deletion Impairs the Early Periosteal Response during Fracture Healing.** It is well known that periosteal stem cells are the major contributors to bone healing and that their ability to give rise to osteoblasts is critical for bone repair (17, 19–21, 24). Ctsk-lineage PSCs contribute to fracture repair (17); thus, our findings that Ctsk-lineage PSCs isolated from *GFP*$^+$*Sfrp4*$^{-/-}$ mice show impaired osteo-chondro differentiation are of importance. Additionally, GO analysis of down-regulated genes identified biological functions related to skeletal development, wound healing, and regulation of mineralization (Tables 1 and 2). We therefore asked whether *Sfrp4* affects the periosteal response to bone fracture. Here, we focused on the early periosteal response and collected mice 5 d after fracture (Fig.6*A*). We found that *Sfrp4* deletion results in impaired periosteal response to fracture as indicated by a decrease in periosteal thickening and impaired cartilaginous callus formation in both males and females (Fig. 6*B* and *SI Appendix*, Fig. S5). We then asked whether this reduced periosteum response conceded with impaired Ctsk-lineage cell response. First, we confirmed that 5 d after femur fracture, GFP$^+$ periosteal cells make a significant contribution to the periosteal response in control animals (Fig. 6*C*) and were present in the

Table 1. GO BP significantly regulated in *GFP⁺Sfrp4⁻/⁻* PSCs vs. *GFP⁺* PSCs

GO:ID	Description	*P* value	*P* adj
GO BP significantly up-regulated in *GFP⁺Sfrp4⁻/⁻* PSCs			
GO:0140014	Mitotic nuclear division	3.40E−08	9.36E−05
GO:0000280	Nuclear division	1.21E−07	0.00016634
GO:0048285	Organelle fission	8.53E−07	0.00078241
GO:0007059	Chromosome segregation	7.04E−06	0.00223586
GO:0000226	Microtubule cytoskeleton organization	1.36E−05	0.00340303
GO:0051783	Regulation of nuclear division	4.58E−05	0.00663457
GO:0022409	Positive regulation of cell-cell adhesion	0.0001135	0.01437572
GO:0007051	Spindle organization	0.0001743	0.02086645
GO:0090068	Positive regulation of cell cycle process	0.0002424	0.02779786
GO:0009612	Response to mechanical stimulus	0.0002980	0.0287589
GO BP significantly down-regulated in *GFP⁺Sfrp4⁻/⁻* PSCs			
GO:0030198	Extracellular matrix organization	3.29E−08	7.41E−05
GO:0030199	Collagen fibril organization	1.58E−07	0.00011844
GO:0002062	Chondrocyte differentiation	2.14E−06	0.00060265
GO:0051216	Cartilage development	1.90E−05	0.00240902
GO:0090287	Regulation of cellular response to growth factor stimulus	3.63E−05	0.00340416
GO:0001501	Regulation of nuclear division	4.58E−05	0.00663457
GO:0022409	Skeletal system development	4.59E−05	0.00412837
GO:0042060	Wound healing	0.00025638	0.0151805
GO:0051604	Skeletal system morphogenesis	0.00077323	0.02856003
GO:0030501	Positive regulation of bone mineralization	0.00397904	0.07651997

periosteum around the fracture site and in the cartilaginous callus (Fig. 6*C*). However, this response was markedly impaired in *GFP⁺Sfrp4⁻/⁻* mice as indicated by lack of expansion of GFP⁺ (Ctsk⁺) cells (Fig. 6*C*). These findings therefore suggest that *Sfrp4* global deletion impairs the early periosteal response and affects the Ctsk-lineage periosteal cell response to wound healing.

PTH-Induced Periosteal Response Requires Sfrp4. *Sfrp4* is known to be regulated by PTH in OBs and cortical bone (41, 42). Given the known anabolic effect of PTH, the finding that Ctsk-lineage PSCs express the PTH receptor (*Pth1r)* is significant (Fig. 7*A*). To assess the possibility that Sfrp4 contributes to the cortical bone response to PTH(1–34), we treated *GFP⁺;Sfrp4⁻/⁻* and *GFP⁺*female mice with 100 μg/kg/d of human recombinant PTH(1–34) or sterile saline (vehicle) 5d/wk for a 4-wk period starting at 6-wk of age (Fig. 7*B*). Ctsk-lineage PSCs, PP1, and PP2 cells were isolated by flow cytometry 24 h after the last injection. As shown in Fig. 7*C*, PTH(1–34) did not significantly affect the % of total GFP⁺ periosteal cells in either *GFP⁺ or GFP⁺;Sfrp4⁻/⁻* mice. However, we found that while PTH(1–34) significantly increased the % of Ctsk-lineage PSCs in *GFP⁺* mice, no changes were observed in PTH(1–34)-treated *GFP⁺;Sfrp4⁻/⁻* mice (Fig. 7*C*). While, the % of PP1 and PP2 population was significantly increased in the *GFP⁺;Sfrp4⁻/⁻* mice compared to *GFP⁺* mice, PTH(1–34) treatment did not affect the pool of these cells. Similarly, PTH(1–34) treatment did not affect the % of Thy1.2⁺ osteo-chondro lineage cells in either *GFP⁺;Sfrp4⁻/⁻* nor *GFP⁺* mice (Fig. 7*C*). μCt analysis confirmed that *Sfrp4* deletion leads to decreased Ct.BV/TV and Ct.Th and increased Ma.Ar. compared

Table 2. Reactome pathways significantly regulated in *GFP⁺Sfrp4⁻/⁻* PSCs vs. *GFP⁺* PSCs

Reactome:ID	Description	*P* value	*P* adj
Reactome pathways significantly upregulated in *GFP⁺Sfrp4⁻/⁻* PSCs			
R-MMU-68886	M phase	3.33E−07	3.92E−05
R-MMU-69620	Cell cycle checkpoints	5.47E−07	4.82E−05
R-MMU-2559586	DNA damage/telomere stress induced senescence	6.25E−06	0.00020135
R-MMU-2559583	Cellular senescence	1.96E−05	0.00049528
R-MMU-453276	Regulation of mitotic cell cycle	0.00173184	0.01852539
Reactome pathways significantly downregulated in *GFP⁺Sfrp4⁻/⁻* PSCs			
R-MMU-1474244	Extracellular matrix organization	3.03E−08	3.56E−06
R-MMU-1474290	Collagen formation	2.37E−07	9.29E−06
R-MMU-1650814	Collagen formation	4.41E−06	9.43E−05
R-MMU-3000171	Non-integrin membrane-ECM interactions	4.27E−05	9.43E−05
R-MMU-1566948	Elastic fiber formation	0.00102815	0.013423

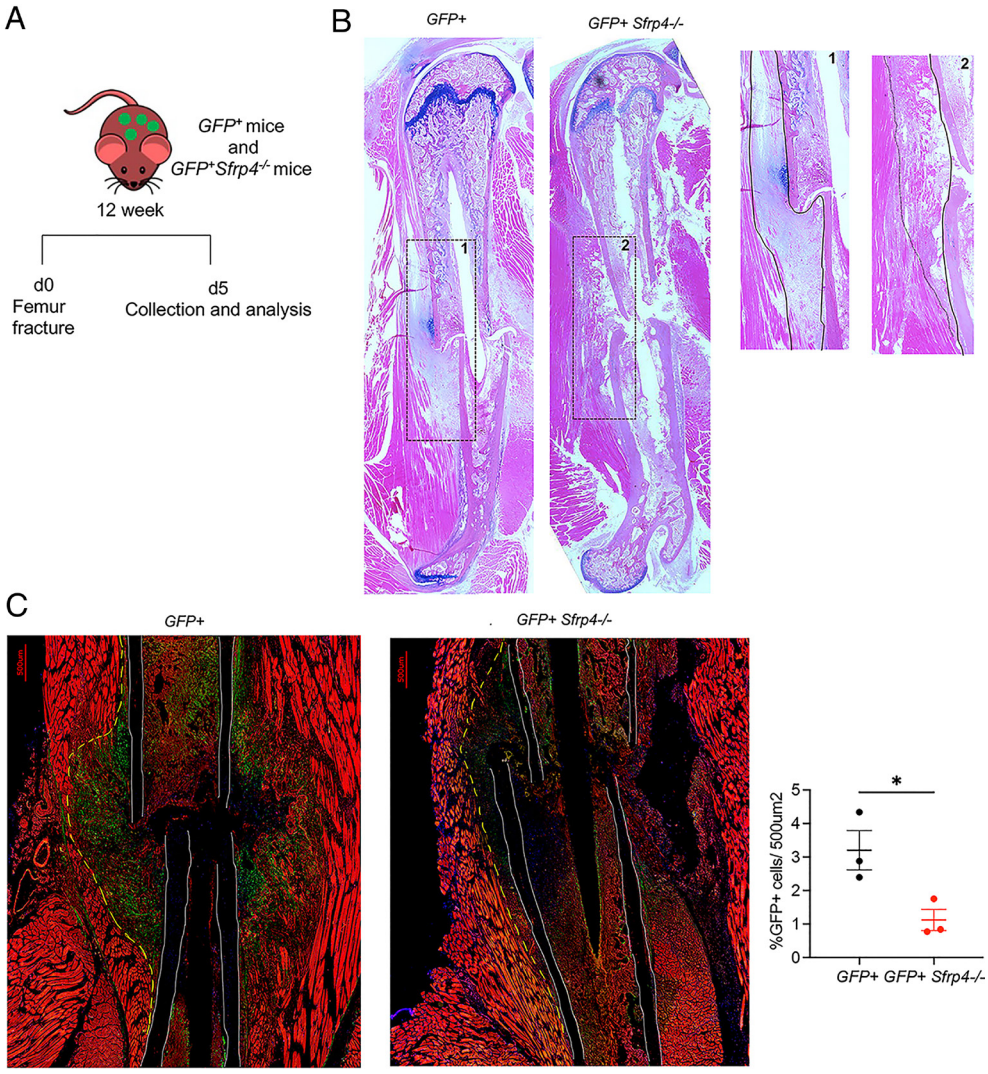

Fig. 6. *Sfrp4* deletion impairs Ctsk-lineage periosteal cell response to fracture. (*A*) Method. (*B*) Representative images of Alcian blue staining of the femur 5 d after fracture in *GFP*$^+$ and *GFP*$^+$*Sfrp4*$^{-/-}$male mice. Images in b1 and b2 are the magnification of the periosteal response and callus formation. Black lines highlight the periosteal response (n = 3 to 6). (*C*) Representative images and quantification of the % of GFP$^+$ cells/500 μm^2. White lines highlight the cortical bone, and yellow dotted lines highlight the periosteal response. Data are expressed as mean ± SEM. *$P < 0.05$ by the Student *t* test (n = 3). (Scale bar, 500 μm.)

to *GFP*$^+$ mice (8). While the treatment significantly increased Ct.BV/TV, Ct.Th in *GFP*$^+$mice, this response was impaired in*GFP*$^+$;*Sfrp4*$^{-/-}$ mice (Fig. 7*D*). Bone histomorphometry analysis on tibia cross-sections confirmed a significant PTH(1–34)-dependent increase in Ps.MS/BS and Ps.BFR/BS in *GFP*$^+$ but not *GFP*$^+$;*Sfrp4*$^{-/-}$ mice (Fig. 7 *D–F* and Table 3).

Discussion

The periosteum is the source of a functionally distinct set of stem cells and progenitors, which contribute to bone homeostasis, have regenerative capacities, and respond to anabolic drugs. Cortical expansion, thickness, and porosity are critical determinants of bone strength in several species including humans (8, 16, 24, 43–48). Given these critical roles, investigations focused on broadening and deepening our understanding of how periosteal stem cells are supported in their niche, and how their differentiation and function are regulated are warranted.

We have previously shown that *Sfrp4* deletion leads to an increase in endosteal resorption and that Sfrp4 regulates endosteal resorption via the Ror2-jnk signaling pathway (14). Here, we show that Sfrp4 is expressed in the periosteum and plays an important role in the multilineage potency, differentiation, and function of a specific population of periosteal cells expressing Ctsk. While it has been elegantly shown that Ctsk marks a subset of periosteal stem cells (PSCs), which fulfill "stemness" criteria, and non-stem cells (PP1 and PP2) (17), the local factors and signaling cues regulating these cells have not been explored extensively. We show that *Sfrp4* deletion leads to a significant decrease in the pool of Ctsk-lineage PSCs, while increasing the % of Ctsk-lineage PP2 cells, and to a decrease in the % of Ctsk-lineage Thy1.2$^+$ osteo-chondro progenitor cells. This outcome results from both suppression of the pool of Ctsk-PSCs and the accumulation of periosteal non-stem progenitors with impaired capability to differentiate into chondrocytes and osteoblasts in vitro. Importantly, by using the renal transplantation assay, we further demonstrate the effect of *Sfrp4* deletion on the vivo capabilities of bone-forming stem cells without prior in vitro expansion.

Several studies using lineage markers such as Prx1, αSMA, Mx1, Sox9, Gli1, or LepR have identified periosteal cell populations with a role in skeletal growth and homeostasis as well in response to fracture healing (15, 17–19, 25, 26, 28, 29, 49–52). Whether these lineage markers identify the same population of periosteal cells or subpopulations of the same cell population and the relationship of these to Ctsk-lineage cells remain to be established. Importantly, given that the periosteum contains distinct cell subpopulations, stem cell–associated surface markers and functional studies are essential together with lineage markers to identify the potential stem cell nature of cells within the periosteum. Thus, using stem cell surface markers, Debnath et al. have identified Ctsk-lineage periosteal stem cells, Duchamp de Lageneste et al. showed that the

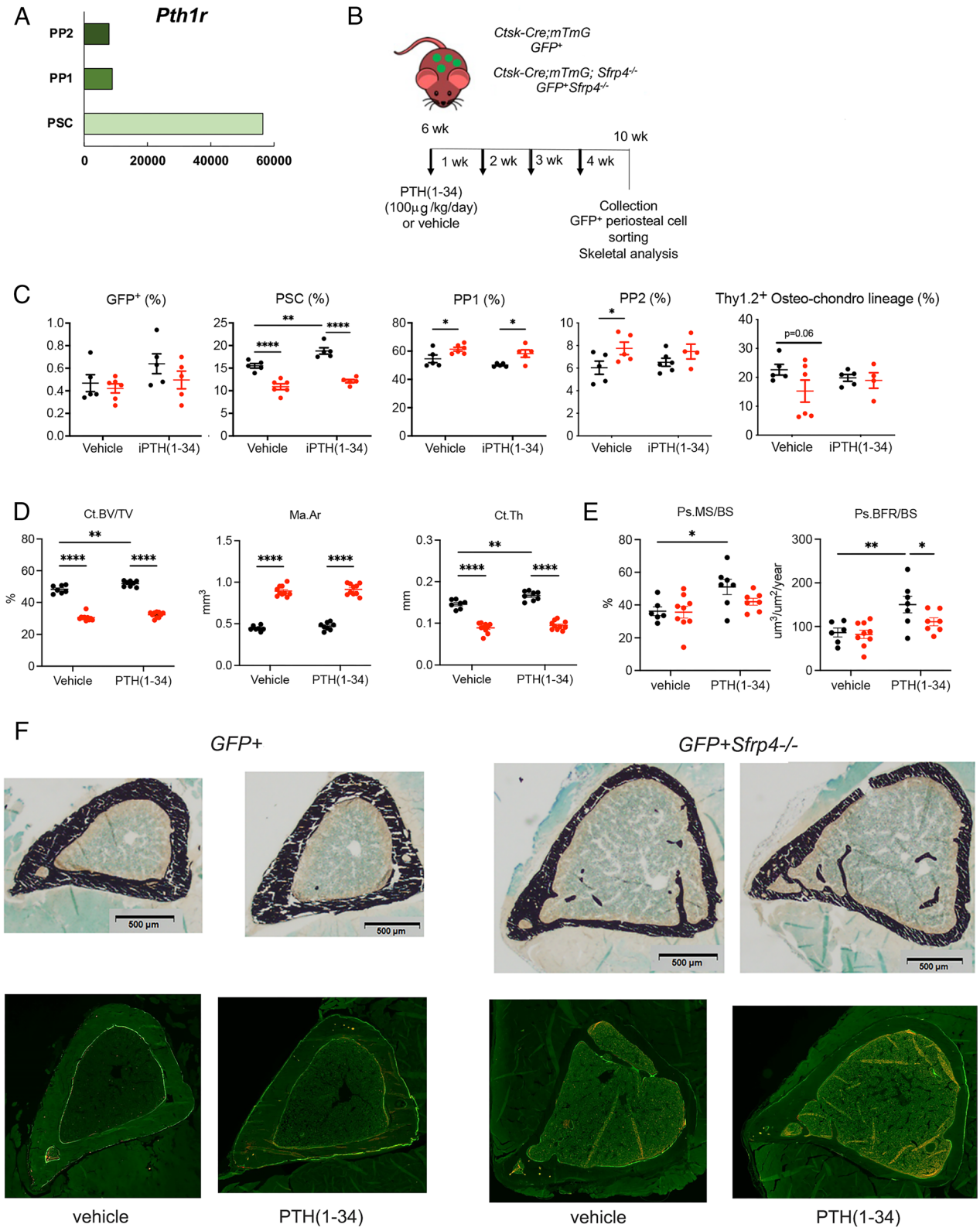

Fig. 7. Response to intermittent PTH is impaired in the absence of *Sfrp4*. (*A*) *Pth1r* expression in Ctsk-lineage PSC, PP1, and PP2 bulk RNA-seq (GSE106237) (17). (*B*) Schematic diagram of PTH(1-34) treatment. (*C*) Percentage of total Ctsk$^+$ cells, Ctsk$^+$ PSC, PP1, PP2, and Thy1.2$^+$ osteochondro-lineage cells in *GFP*$^+$ and *GFP*$^+$*Sfrp4*$^{-/-}$ female mice treated with vehicle or PTH(1-34) (n = 5 to 6). (*D* and *E*) μCT (*D*) and dynamic histomorphometry (*E*) analysis in *GFP*$^+$ and *GFP*$^+$*Sfrp4*$^{-/-}$ mice treated with vehicle or PTH(1-34). (n = 6 to 9). (*F*) Representative images of Von Kossa staining and double labeling in *GFP*$^+$ and *GFP*$^+$*Sfrp4*$^{-/-}$ mice treated with vehicle or PTH(1-34). All data: mean ± SEM, **P* < 0.05, ***P* < 0.01, ****P* < 0.005, and *****P* < 0.001 by two-way ANOVA followed by the Fisher test.

periosteum contains Prx1$^+$ skeletal stem cells, and Guo et al showed that subsets of periosteal LepR$^+$ cells possess self-renewal capacity and commit to osteogenic lineage cells (17, 18, 52). Here, we focused on Ctsk-lineage cells and while our studies show that Sfrp4 influences the Ctsk-lineage periosteal stem cells, its function in non-Ctsk lineage periosteal cells, which might include some of these alternative markers, cannot be excluded. Ctsk, an enzyme secreted by osteoclasts, digests bone matrix proteins and is critical

Table 3. Histomorphometry analyses of midshaft tibiae

	Vehicle		PTH(1–34)		Two-way ANOVA		
Parameters	*GFP*$^+$ n = 6	*GFP*$^+$; *Sfrp4*$^{-/-}$ n = 9	*GFP*$^+$ n = 7	*GFP*$^+$; *Sfrp4*$^{-/-}$ n = 7	Treatment	Genotype	Interaction
Ct.T.Ar	1.27 ± 0.06	1.9 ± 0.09^A	1.533 ± 0.09^a	2.11 ± 0.038^B	$P = 0.007$	$P < 0.0001$	NS
Ma.Ar.(mm^2)	0.61 ± 0.03	1.31±0.08^A	0.693 ± 0.05	1.41 ± 0.04^B	$P = 0.048$	$P < 0.0001$	NS
Ct.BV/TV (%)	51.5 ± 1.43	31.22±1.26^A	54.53 ± 0.95	32.9 ± 0.96^B	NS	$P < 0.0001$	NS
Ct.Th (mm)	155 ± 6.4	108.2 ± 4.71^A	1763 ± 16.34^A	120.14 ± 4.76^B	$P = 0.009$	$P < 0.0001$	NS
Ps.MS/BS(%)	38 ± 2.71	35.5 ± 3.54	51.13 ± 4.64^A	41.9 ± 2.14	$P = 0.006$	NS	NS
Ps.MAR (μm/day)	0.67 ± 0.14	0.64±0.04	0.83 ± 0.04^A	0.72 ± 0.05	$P = 0.012$	NS	NS
Ps.BFR/BS (μm^3/μm^2/day)	90.7 ± 7.68	82.4 ± 9.22	150.43 ± 19^A	110.8 ± 9.26^b	$P = 0.011$	NS	NS

Data are expressed as Mean ± SEM. Two-Way ANOVA followed by Fisher's LSD test. a = $P < 0.05$ and A = $P < 0.01$ compared to *GFP*+ Vehicle-treated mice b = $P < 0.05$ and B = $P < 0.01$ compared to PTH(1-34)-treated mice.

for bone resorption (31–33, 53, 54). Ctsk mutations in humans lead to pycnodysostosis a disease characterized by osteosclerosis, skeletal deformities, short stature, and brittle bones (53, 55). Pycnodysostosis patients present with high trabecular bone and tick cortical bone. While high trabecular bone is mainly due to a decrease in bone resorption, high cortical thickness is due to increased periosteal formation (53). Ctsk deletion in mice or treatment with the Ctsk inhibitor odanacatib leads to a similar phenotype (31, 32, 56–60). Thus, although it might be surprising to find Ctsk-lineage cells in the periosteum, these observations support a role for Ctsk in the periosteum and may account for the effect seen upon treatment with the Ctsk inhibitor odanacatib at the periosteal surface (59). Ctsk-lineage periosteal cells play an important role in cortical bone homeostasis as deletion of *osterix*, a transcription factor required for osteoblast differentiation (61), in Ctsk-lineage cells leads to cortical bone thinning, increased porosity, and fracture risk (17). Additionally, recent studies have shown a role for Ctsk-lineage periosteal cells in the Ihh-signaling pathway in the growth plate (62). The finding that Ctsk controls cortical bone formation by degrading periostin, a matricellular protein critical for Wnt- and PTH- mediated periosteal bone formation (63) might explain the cortical and periosteal phenotype. However, the mechanisms by which periosteal bone formation, which occurs through modeling (24, 46, 64) is increased in the absence of Ctsk, remain unclear.

Osteocytes can also express Ctsk under certain circumstances (65, 66), however, deletion of Ctsk in mature osteoblasts and osteocytes does not alter cortical or cancellous bone under steady-state conditions although it prevented the loss of cancellous bone induced by lactation (65), suggesting an osteocyte-independent role of Ctsk on the regulation of periosteal homeostasis.

The absence of *Sfrp4* leads to a significant decrease in the pool of Ctsk-lineage PSCs, enhanced differentiation toward the PP2 cell population, and impaired ability to give rise to Thy1.2$^+$ osteo-chondro progenitors. Interestingly, the ability of PP1 and PP2 cells to give rise to Thy1.2$^+$ osteo-chondro progenitors was also significantly impaired by *Sfrp4* deletion. Additionally, we show that *Sfrp4* deletion significantly affects in vitro clonal multipotency for differentiation into osteoblasts and chondrocytes of Ctsk-lineage PSCs, PP1, and PP2 cells. Similar results were also seen in a kidney capsule transplantation. Given that Sfrp4 is predominantly expressed by Ctsk-lineage PP1 and PP2 cells, the phenotype seen in PSCs isolated from *GFP*$^+$*Sfrp4*$^{-/-}$ mice might be, at least in part, due to *Sfrp4* deletion in PP1 and/or PP2 cells. Indeed, given that PSCs in culture give rise to their PP1 and PP2 derivatives, we cannot exclude paracrine/autocrine feedback loop between Ctsk-lineage PSCs, PP1, and PP2 cells present in these cultures. Interestingly, our study suggests that Sfrp4 might have a role in Ctsk-lineage periosteal cell fate decision, by favoring their commitment and differentiation along the osteo-chondro and osteoblast lineage while retaining them from differentiating into the adipogenic lineage as shown by our findings that while in vitro Ctsk-lineage cells do not form adipocyte colonies but do so in the absence of *Sfrp4*. Although we do not suggest that adipocytes are present in the periosteal surface of *Sfrp4*-deficient mice, these findings indicate the complexity of Sfrp4-mediated signaling and its role in inhibiting Ctsk-lineage periosteal cells from differentiating into adipocytes and for retaining their ability to properly committee to the osteoblast lineage.

Given the known role of Wnt signaling in the regulation of cortical bone appositional growth and homeostasis (2, 8, 45), it is not surprising that Ctsk-lineage periosteal stem cells and non-stem progenitors express several components of the Wnt signaling machinery, although at different levels (17). Interestingly, we noted that Wnt components classically associated with noncanonical Wnt cascades, such as *Wnt4*, *Wnt5a*, *Wnt5b*, *Wnt11*, *c-jun*, and *Ryk,* were generally strongly expressed in these cells (2, 8, 14, 44), while canonical ligands such as *Wnt1* and *Wnt3a* or downstream target genes such as *Axin2*, *Dkk1,* and *Lef1* were not (7). Thus, it is plausible that paracrine and autocrine signaling and feedback loop mechanisms among PSCs, PP1, and PP2 cell populations regulate their expansion and function mostly through noncanonical Wnt signaling, such that specific downstream signaling cascades may be activated in the absence of *Sfrp4*, strengthen our previous observations in the cortical bone of *Sfrp4*$^{-/-}$ mice (8, 14). Excluding an overall change in Wnt ligand expression in the absence of *Sfrp4,* our RNA-seq analysis shows that among the Wnt ligands, only Wnt4, which has been shown to positively regulate osteoblast differentiation (67), was significantly down-regulated in Ctsk-lineage PSCs isolated from the Sfrp4 null mice, while no significant changes in the level of expression of Wnt receptor/coreceptor were observed. The findings that *Sfrp4* deletion does not result in significant changes in ligand, receptor/coreceptor expression, support the notion that given that Sfrp4 functions as a Wnt ligand decoy receptor, its function in skeletal homeostasis is related to the regulation of distinct Wnt signaling pathways more than to the regulation of the expression of Wnt ligands, frizzled receptors, and coreceptors it engages with.

We also found that several genes and signaling pathways associated with skeletal morphogenesis, extracellular matrix, collagens, and repair were significantly down-regulated in PSCs isolated from *GFP*$^+$*Sfrp4*$^{-/-}$ mice. Sirius red staining indicates that lack of *Sfrp4* leads to a disorganization of collagen fibrils in cortical bone and fracture experiments show that lack of *Sfrp4* hinders the periosteal response to bone fracture and callus formation and this was associated with a decrease in the Ctsk-lineage cells. Previous studies

have reported that Col2a1$^+$ cells in bone marrow, growth plate and perichondrial/periosteal are skeletal stem cells, and genetic lineage tracing studies, have recently shown that embryonic Col2a1$^+$ cells contribute to cells in the growth plate, trabecular or cortical bone, tendons, and ligaments (68–72). Our findings that Col2a1 expression is decreased in *Sfrp4*-deficient Ctsk-lineage PSCs, are therefore consistent with our hypothesis that absence of *Sfrp4* negatively affects the differentiation and functionality of these cells.

Although we are aware that our studies do not exclude the possibility that non-Ctsk expressing cells in the periosteum might also be affected by *Sfrp4* deletion, we clearly show that the GFP$^+$ (Ctsk$^+$) cells are significantly decreased in *Sfrp4*$^{-/-}$ fractured bones compared to control mice. It is known that individuals with Pyle disease present with increased risk fracture. These fractures tend to be "unusual" because of the particular shape of the long bones in these individuals (8, 73, 74), and thus, bone repair could be slower. There is one clinical case reporting normal fracture repair, but this was only a follow-up after 2 y, and no data of early repair process were documented (75). On the other hand, old pathological fracture with exuberant callus and bone remodeling defect were reported in another case of Pyle disorder (76). However, given that 1) fracture healing is often variable in healthy individuals and 2) there are not enough cases of Pyle disease (less than 50 worldwide) reported as today, we cannot conclude from clinical data alone that fracture healing in individuals with Pyle disease would be impaired. Nonetheless, our findings in mice suggest that in the absence of *Sfrp4*, the periosteal responses to bone fractures are significantly impaired.

Bulk RNA-seq analysis shows that a few cell-cycle associated genes and biological pathways related to cell cycle regulation are up-regulated in PSCs isolated from *Sfrp4*$^{-/-}$ mice, although PSC proliferation was not significantly affected by *Sfrp4* deletion. Interactions between the cell cycle machinery and differentiation factors play a critical role in stem cell maintenance, proliferation, and differentiation (77–79). However, how the crosstalk between cell cycle proteins and growth factors affects stemness, proliferation, or lineage-restricted differentiation remains elusive. It is plausible that in the absence of *Sfrp4*, although a few cyclins are up-regulated, the balance between growth factors and cell cycle proteins does not reach the threshold to tilt toward proliferation but favors differentiation.

Sfrp4 was initially identified as a target gene of PTH signaling (42, 80–82). The findings that Ctsk-lineage PSCs express high levels of *Pth1r* (17) raise the possibility that these cells are mediators of the anabolic effect of PTH in the periosteum (22, 23) and that Sfrp4 contributes to the cortical bone response to PTH(1–34). Supporting this hypothesis, we found that the PTH-dependent increase in cortical thickness, periosteal mineral apposition rate and bone formation rate were significantly impaired in the absence of *Sfrp4* and that PTH treatment at the dose of 100 μg/kg for 5 d/wk for 4 wk, leads to an increase in the Ctsk-lineage PSC %, a response not seen in the absence of *Sfrp4*.

Limitations of the Study

We are aware that using a mouse model with global deletion of Sfrp4 might complicate some of our interpretations and conclusions. Thus, we recognize that our study does not fully exclude a developmental effect that might "imprint" on the Ctsk-lineage cells and/or that cells might maintain a memory of their in vivo milieu. However, the fact that our flow cytometry/FACS studies characterize and sort the Ctsk-lineage cells using an extensive and known panel of stem cell markers should reduce the risk that the differences observed are associated with uncharacterized changes in the Ctsk-lineage periosteal cell subpopulations.

We are also aware that deletion of *Sfrp4* in other bone cells (osteoblasts/osteocytes/osteoclasts) or Ctsk-negative periosteal cells might influence periosteal cell expansion, differentiation, and function in their native setting. However, our studies, showing clear composition and functional differences between cells isolated from *GFP*$^+$ and *GFP*$^+$*Sfrp4*$^{-/-}$ mice and cultured in vitro up to 14 d or transplanted in vivo for 3 wk, were performed using only immunophenotypic Ctsk-lineage cells and thereby support an intrinsic effect of Sfrp4 on their behavior. Similarly, while our fracture studies demonstrate that *Sfrp4* global deletion impairs fracture healing and decreases the pool of Ctsk-lineage cells in the periosteum, our studies do not exclude that this might be also associated with the impaired function of Ctsk-negative periosteal cells or other "first responder" cells lacking *Sfrp4*. Finally, based on the fact that Pth1r is expressed in osteocytes and that the anabolic effects of PTH are largely due to its effects on the osteocytes (83–85), our data do not exclude that the impaired cortical response to PTH seen in the absence of *Sfrp4* might be due to defects in the osteocytes which could also indirectly affect the Ctsk-lineage periosteal cells. Nonetheless, our studies support the hypothesis that Sfrp4 might be a downstream effector of PTH signaling in cortical bone.

While data obtained from the Sfrp4 global knockout model are precious, especially when thinking about human skeletal disorders such as Pyle disease, studies focused to explore the role of Sfrp4 in specific bone cells will be required to further the investigations presented here. Specific targeted deletion of *Sfrp4* in these cells is needed to provide important mechanistic insights into the direct effects of Ctsk-lineage periosteal-secreted Sfrp4.

Conclusions

In summary, the periosteum is a major source of stem cells and progenitors, contributes to bone homeostasis, has regenerative capacities, and responds to anabolic drugs. Analysis of signaling molecules and pathways regulating periosteal stem cells and progenitors provides an outstanding opportunity to advance our understanding of the mechanisms involved in these processes and may provide specific therapeutic options for human diseases associated with bone fragility and impaired bone healing and bone regeneration. Overall, our studies identify Sfrp4, a soluble Wnt antagonist, as a critical regulator of the number and distribution across the various subpopulations of Ctsk-lineage periosteal stem cells/progenitors as well as of their function. We show that PTH regulates these specific pools of periosteal cells and that Sfrp4 is a potential downstream effector of PTH in the periosteum. Highlighting the significance of further investigating bone healing mechanisms, our studies support the hypothesis that Sfrp4 is required for the periosteal response to fractures and for Ctsk-lineage periosteal cells to be activated in bone repair.

Materials and Methods

Biological Variables and Reproducibility. To conduct the proposed studies, we used strict application of scientific methods that support robust and unbiased design, analysis, interpretation, and reporting of results, and sufficient information for all studies undertaken. In vivo analyses, with the exception of the PTH(1–34) treatment, were performed in males and females. *Sfrp4* global knockout, *CtskCre;mTmG;wt* (GFP$^+$) and *CtskCre;mTmG;Sfrp4*$^{-/-}$ (GFP$^+$;Sfrp4$^{-/-}$) mice were investigated. To avoid bias, data were collected in a blinded fashion, in that the observer was unaware of the experimental groups and more than one individual performed key studies. In vivo studies were performed with n = 3 to 9 mice per genotype. We based this number on a priori calculations as detailed in *SI Appendix*. Ex vivo and in vitro studies involved at least three biological replicates per group/treatment.

Animals. *Sfrp4* null mice were previously described (8, 14). *CtskCre* mice were kindly provided by S. Kato, University of Tokyo, Tokyo, Japan, and *Rosa26*$^{mT/mG}$ mice (Stock 007676) were purchased from Jackson Laboratories. *CtskCre;mTmG;Sfrp4*$^{-/-}$ (*GFP*$^{+}$*;Sfrp4*$^{-/-}$) and *CtskCre;mTmG;wt* (GFP^{+}) mice were obtained as detailed in *SI Appendix*. To examine the effect of PTH(1–34) (Tocris Bio-Techne Corporation), mice were given subcutaneous injections 5 d/wk of vehicle (100 µL 0.9% saline solution) or 100 µg/kg body weight of PTH(1–34) for 4 wk. See *SI Appendix* for more details.

RNAscope. Tibiae isolated from 4- to 5-wk-old wild-type (*WT*) and *Sfrp4*$^{-/-}$ mice were fixed with 4% paraformaldehyde (PFA). Samples were prepared as detailed in *SI Appendix*. *Sfrp4* mRNA localization was performed using RNAScope according to the manufacturer's protocol (RNAscope Probe-Mm-Sfrp4 # 404991 and Probe-Mm-Col1a-1#1319371-C4, Advanced Cell Diagnostics). Images in the diaphysis of cortical bone were taken using the Leica MZFLIII Microscope.

Periosteum Culture. Microdissection of the mouse long bone periosteum from 4-wk-old *GFP*$^{+}$*;Sfrp4*$^{-/-}$ and *GFP*$^{+}$ mice was performed under a dissecting microscope as previously reported (17) and as detailed in *SI Appendix*. Cells were counted, replated at a 5,000/cm^2 density, and cultured as detailed in *SI Appendix*.

Periosteum Isolation, Fluorescence-Assisted Cell Sorting (FACS), and Flow Cytometry. The periosteum was isolated as described above from both long bones and calvariae. Samples were centrifuged, resuspended in ice-cold FACS buffer (2% FBS + 1 mM EDTA in PBS), and filtered through 70-µm nylon mesh. Cells were then centrifuged, resuspended in ice-cold FACS buffer and incubated with blocking buffer (1:100 dilution; BD Biosciences 553142 for mouse) for 10 min at 4 °C. Antibodies for flow cytometry and FACS analysis are reported in *SI Appendix*. FACS and flow cytometry studies were performed as detailed in *SI Appendix*. PSCs (CD45$^-$CD31$^-$Ter119$^-$(Lin$^-$)Thy1.2$^-$6C3$^-$GFP$^+$CD105$^-$ CD200$^+$) and their derivate progenitor cells, PP1 (Lin$^-$ Thy1.2$^-$6C3$^-$GFP$^+$CD105$^-$CD200$^-$) and PP2 (Lin$^-$ Thy1.2$^-$6C3$^-$GFP$^+$CD105$^+$CD200^{variable}), cells were investigated.

Culture of Sorted Ctsk-Lineage PSC, PP1, and PP2 Cells. Sorted PSCs (CD45$^-$CD31$^-$Ter119$^-$(Lin$^-$)Thy1.2$^-$6C3$^-$GFP$^+$CD105$^-$ CD200$^+$) and their derivate progenitor cells, PP1 (Lin$^-$Thy1.2$^-$6C3$^-$GFP$^+$ CD105$^-$ CD200$^-$) and PP2 (Lin$^-$Thy1.2$^-$6C3$^-$GFP$^+$CD105$^+$CD200^{variable}) cells, were cultured in complete culture medium under hypoxic (2% O_2, 10% CO_2, 88% N_2) conditions. Half of the medium was replaced every 3 d. Cells were passaged once they were 60 to 70% confluent with trypsin (Gibco, A11105-01). To assess clonal multipotency of Ctsk-lineage cells, sorted PSCs, PP1, and PP2 cells were allowed to form individual colonies. At least 10 single colonies were isolated using a cloning cylinder. Single colonies were expanded and then reanalyzed by flow cytometry using the same panel of antibodies described above or differentiated without or with osteogenic, adipogenic, or chondrogenic conditions as detailed in *SI Appendix*.

Kidney Capsule Transplantation. Eight–ten-week-old WT male mice were anesthetized and shaved on the left flank and abdomen before sterilization of the surgical site. Recipients for these experiments were syngeneic with donors. A 5-µL Matrigel plug (Corning, 356231) containing 8,000 to 10,000 sorted Ctsk-lineage PSCs, PP1, or PP2 cells was implanted underneath the renal capsule. Animals were killed by CO_2 after 3 wk. Kidneys were fixed with 4% PFA for 5 h and subjected to infiltration, embedding, and sectioning. Von Kossa (Sigma-Aldrich) staining was performed to detect mineralized nodule formation. Quantification of Von Kossa staining was performed using Image J (NIH.gov, version 1.53t).

Cell Proliferation. To evaluate cell proliferation in vivo, 5-ethynyl-2′-deoxyuridine (EdU) (Invitrogen, C10634) was dissolved in phosphate-buffered saline (PBS) and administered (200 µg) 12 h before killing. Ctsk-lineage periosteal cells were isolated as described above, and cell proliferation was detected using the Click-iT EdU Alexa Flour 350 Assay kit (Invitrogen, C10634). Edu$^+$ Ctsk-lineage PSCs, PP1, and PP2 cells were then detected by using flow cytometry as described above.

Bulk RNA Sequencing. Bulk RNA-seq was performed on sorted Ctsk-lineage PSC, isolated from 4-wk-old mouse femurs and tibiae. Three mice/genotype were pooled for each RNA sample submitted for bulk RNA-seq. RNA was isolated using the microQiagen kit (Qiagen) following the manufacturer's instructions. Library, sequencing, and analysis were performed by Novogene Corporation, Inc., as detailed in *SI Appendix*.

Fracture Experiments. For fracture studies, surgery was performed on 12-wk-old mice as previously described (86) and as detailed in *SI Appendix*. For histological analysis**,** paraffin and frozen sections were prepared, stained, and imaged as detailed in *SI Appendix*. Quantification of GFP$^+$ cells was performed using Image J (NIH.gov, version 1.53t). The ROI (500 µm × 500 µm square) measured was positioned right above the fracture site, and the area covered by GFP$^+$ cells within the ROI was calculated for each image.

Picro Sirius Red Staining. Tibiae isolated from 4- to 5-wk-old *wt* and *Sfrp4*$^{-/-}$ mice were fixed with 4% PFA. Samples were decalcified following the manufacturer's protocol (Advanced Cell Diagnostics, Newark, CA, # 322300), embedded in paraffin and 10 to 20 µm in thickness sections cut. Picro Sirius Red staining was performed using the Picro Sirius Red Stain Kit (Connective Tissue Stain, Abcam ab150681) according to the manufacturer's protocol. Images in the diaphysis of cortical bone were obtained using the Leica MZFLIII Microscope.

Skeletal Phenotype. For bone histomorphometry analysis, mice were injected and sessions prepared, stained, and viewed as detailed in *SI Appendix*. OsteoMeasure analyzing software (OsteoMetrics Inc.) was used to generate and calculate the data (*SI Appendix*). All the parameters were obtained blindly and presented according to the standardized nomenclature (87).

For microcomputed tomography (µCT) scanning, a high-resolution desktop microtomographic imaging system (µCT35, Scanco Medical AG, Brüttisellen, Switzerland) was used to assess cortical bone morphology as described in *SI Appendix*. Image acquisition and analysis protocols adhered to the JBMR guidelines (88).

Statistical Analysis. Statistical analyses were performed using GraphPad Prism 9 software. For flow cytometry analysis and CFU studies, statistical significance was determined by an unpaired two-tailed Student *t* test. For µCT studies, statistical significance was determined by a two-way ANOVA followed by Tukey's multiple comparisons test to detect differences between groups. A *P* value of less than 0.05 was considered statistically significant. Outcomes were reported as means ± SE otherwise indicated. The number of samples per group is indicated in the figure legends.

Data, Materials, and Software Availability. Bulk-RNA sequencing data have been deposited in GEO repository (GSE236686) (37).

ACKNOWLEDGMENTS. This work was supported by grants from the NIH-NIDCR R56DE028299 (F.G.), R01DE029615 (F.G.), and in part from the Milton Fund, Office of the Vice Provost for Research Harvard University (F.G.). We would like to thank Dr. Superti-Furga for his insights into the fracture repair in individuals with Pyle disease.

Author affiliations: [a]Division of Bone and Mineral Research, Department of Oral Medicine, Infection and Immunity, Harvard School of Dental Medicine, Boston, MA 02115; [b]Department of Cancer Immunology and Virology, Dana-Farber Cancer Institute and Harvard University Medical School, Boston, MA 02115; [c]Department of Developmental Biology, Harvard Medical School and Harvard School of Dental Medicine, Boston, MA 02115; [d]Harvard Medical School, Department of Medicine, Endocrine Unit, Massachusetts General Hospital, Boston, MA 02114; [e]Department of Pathology and Laboratory Medicine, Weill Cornell Medicine, New York, NY 10065; and [f]Research Division, Hospital for Special Surgery, New York, NY 10021

1. C. M. Cruciat, C. Niehrs, Secreted and transmembrane wnt inhibitors and activators. *Cold Spring Harb Perspect Biol.* **5**, a015081. (2013).
2. F. Gori, R. Baron, "Wnt signaling in skeletal homeostasis and diseases" in *Osteoporosis*, D. W. Dempster, J. A. Cauley, M. L. Bouxsein, F. Cosman, Eds. (Academic Press, Elsevier, ed. 5, 2021), pp. 257–279.
3. H. Guan *et al.*, Secreted frizzled related proteins in cardiovascular and metabolic diseases. *Front. Endocrinol. (Lausanne)* **12**, 712217 (2021).
4. C. J. Liang *et al.*, SFRPs are biphasic modulators of wnt-signaling-elicited cancer stem cell properties beyond extracellular control. *Cell Rep.* **28**, 1511–1525.e1515 (2019).
5. P. Bovolenta, P. Esteve, J. M. Ruiz, E. Cisneros, J. Lopez-Rios, Beyond Wnt inhibition: New functions of secreted Frizzled-related proteins in development and disease. *J. Cell Sci.* **121**, 737–746 (2008).
6. N. M. Pawar, P. Rao, Secreted frizzled related protein 4 (sFRP4) update: A brief review. *Cell Signal* **45**, 63–70 (2018).

7. R. Baron, M. Kneissel, WNT signaling in bone homeostasis and disease: From human mutations to treatments. *Nat. Med.* **19**, 179–192 (2013).
8. P. O. Simsek Kiper *et al.*, Cortical-bone fragility-insights from sFRP4 deficiency in Pyle's disease. *N. Engl. J. Med.* **374**, 2553–2562 (2016).
9. N. Chatron *et al.*, A novel homozygous truncating mutation of the SFRP4 gene in Pyle's disease. *Clin. Genet.* **92**, 112–114 (2017).
10. C. Galada, H. Shah, A. Shukla, K. M. Girisha, A novel sequence variant in SFRP4 causing Pyle disease. *J. Hum. Genet.* **62**, 575–576 (2017).
11. A. Sowinska-Seidler *et al.*, The first report of biallelic missense mutations in the SFRP4 gene causing Pyle disease in two siblings. *Front Genet.* **11**, 593407 (2020).
12. R. Brommage, J. Liu, D. R. Powell, Skeletal phenotypes in secreted frizzled-related protein 4 gene knockout mice mimic skeletal architectural abnormalities in subjects with Pyle's disease from SFRP4 mutations. *Bone Res.* **11**, 9 (2023).
13. R. Chen, R. Baron, F. Gori, Sfrp4 and the biology of cortical bone. *Curr. Osteoporos Rep.* **20**, 153–161 (2022).
14. K. Chen *et al.*, Sfrp4 repression of the Ror2/Jnk cascade in osteoclasts protects cortical bone from excessive endosteal resorption. *Proc. Natl. Acad. Sci. U.S.A.* **116**, 14138–14143 (2019).
15. Y. Cao, E. J. Buckels, B. G. Matthews, Markers for identification of postnatal skeletal stem cells in vivo. *Curr. Osteoporos Rep.* **18**, 655–665 (2020).
16. H. Chang, M. L. Knothe Tate, Concise review: The periosteum: Tapping into a reservoir of clinically useful progenitor cells. *Stem Cells Transl. Med.* **1**, 480–491 (2012).
17. S. Debnath *et al.*, Discovery of a periosteal stem cell mediating intramembranous bone formation. *Nature* **562**, 133–139 (2018).
18. O. Duchamp de Lageneste *et al.*, Periosteum contains skeletal stem cells with high bone regenerative potential controlled by Periostin. *Nat. Commun.* **9**, 773 (2018).
19. B. G. Matthews *et al.*, Heterogeneity of murine periosteum progenitors involved in fracture healing. *Elife* **10**, e58534 (2021).
20. S. J. Roberts, N. van Gastel, G. Carmeliet, F. P. Luyten, Uncovering the periosteum for skeletal regeneration: The stem cell that lies beneath. *Bone* **70**, 10–18 (2015).
21. X. Zhang *et al.*, Periosteal stem cells are essential for bone revitalization and repair. *J. Musculoskelet Neuronal. Interact* **5**, 360–362 (2005).
22. R. L. Jilka, Molecular and cellular mechanisms of the anabolic effect of intermittent PTH. *Bone* **40**, 1434–1446 (2007).
23. R. L. Jilka *et al.*, Intermittent PTH stimulates periosteal bone formation by actions on post-mitotic preosteoblasts. *Bone* **44**, 275–286 (2009).
24. T. Isojima, N. A. Sims, Cortical bone development, maintenance and porosity: Genetic alterations in humans and mice influencing chondrocytes, osteoclasts, osteoblasts and osteocytes. *Cell Mol. Life Sci.* **78**, 5755–5773 (2021).
25. L. C. Ortinau *et al.*, Identification of functionally distinct Mx1+alphaSMA+ periosteal skeletal stem cells. *Cell Stem Cell* **25**, 784–796 e785 (2019).
26. N. Ono, D. H. Balani, H. M. Kronenberg, Stem and progenitor cells in skeletal development. *Curr. Top Dev. Biol.* **133**, 1–24 (2019).
27. T. Mizoguchi *et al.*, Osterix marks distinct waves of primitive and definitive stromal progenitors during bone marrow development. *Dev. Cell* **29**, 340–349 (2014).
28. T. H. Ambrosi, M. T. Longaker, C. K. F. Chan, A revised perspective of skeletal stem cell biology. *Front Cell Dev. Biol.* **7**, 189 (2019).
29. Y. Matsushita, W. Ono, N. Ono, Skeletal stem cells for bone development and repair: Diversity matters. *Curr. Osteoporos Rep.* **18**, 189–198 (2020).
30. E. C. Jeffery, T. L. A. Mann, J. A. Pool, Z. Zhao, S. J. Morrison, Bone marrow and periosteal skeletal stem/progenitor cells make distinct contributions to bone maintenance and repair. *Cell Stem Cell* **29**, 1547–1561.e1546 (2022).
31. R. Kiviranta *et al.*, Impaired bone resorption in cathepsin K-deficient mice is partially compensated for by enhanced osteoclastogenesis and increased expression of other proteases via an increased RANKL/OPG ratio. *Bone* **36**, 159–172 (2005).
32. B. Pennypacker *et al.*, Bone density, strength, and formation in adult cathepsin K (−/−) mice. *Bone* **44**, 199–207 (2009).
33. P. Saftig *et al.*, Impaired osteoclastic bone resorption leads to osteopetrosis in cathepsin-K-deficient mice. *Proc. Natl. Acad. Sci. U.S.A.* **95**, 13453–13458 (1998).
34. C. K. Chan *et al.*, Identification and specification of the mouse skeletal stem cell. *Cell* **160**, 285–298 (2015).
35. C. K. F. Chan *et al.*, Identification of the human skeletal stem cell. *Cell* **175**, 43–56.e21 (2018).
36. G. S. Gulati *et al.*, Isolation and functional assessment of mouse skeletal stem cell lineage. *Nat. Protoc.* **13**, 1294–1309 (2018).
37. R. Chen, H Dong, R. Baron, M. B. Greenblatt, F. Gori, Sfrp4 is Required to Maintain Ctsk-Lineage Periosteal Stem Cell Niche Function. GEO. https://www.ncbi.nlm.nih.gov/geo/query/acc.cgi?&acc=GSE236686. Deposited 6 July 2023.
38. H. Choi, C. E. Magyar, J. M. Nervina, S. Tetradis, Different duration of parathyroid hormone exposure distinctively regulates primary response genes Nurr1 and RANKL in osteoblasts. *PLoS One* **13**, e0208514 (2018).
39. M. K. Lee, H. Choi, M. Gil, V. M. Nikodem, Regulation of osteoblast differentiation by Nurr1 in MC3T3-E1 cell line and mouse calvarial osteoblasts. *J. Cell Biochem.* **99**, 986–994 (2006).
40. F. Q. Pirih, T. L. Aghaloo, O. Bezouglaia, J. M. Nervina, S. Tetradis, Parathyroid hormone induces the NR4A family of nuclear orphan receptors in vivo. *Biochem. Biophys. Res. Commun.* **332**, 494–503 (2005).
41. M. K. Bergenstock, N. C. Partridge, Parathyroid hormone stimulation of noncanonical Wnt signaling in bone. *Ann N Y Acad. Sci.* **1116**, 354–359 (2007).
42. X. Li *et al.*, Determination of dual effects of parathyroid hormone on skeletal gene expression in vivo by microarray and network analysis. *J. Biol. Chem.* **282**, 33086–33097 (2007).
43. V. Bousson *et al.*, Distribution of intracortical porosity in human midfemoral cortex by age and gender. *J. Bone Miner Res.* **16**, 1308–1317 (2001).
44. F. Gori, U. Lerner, C. Ohlsson, R. Baron, A new WNT on the bone: WNT16, cortical bone thickness, porosity and fractures. *Bonekey Rep.* **4**, 669 (2015).
45. S. Moverare-Skrtic *et al.*, Osteoblast-derived WNT16 represses osteoclastogenesis and prevents cortical bone fragility fractures. *Nat. Med.* **20**, 1279–1288 (2014).
46. E. Seeman, Periosteal bone formation–a neglected determinant of bone strength. *N. Engl. J. Med.* **349**, 320–323 (2003).
47. E. Seeman, Age- and menopause-related bone loss compromise cortical and trabecular microstructure. *J. Gerontol. A. Biol. Sci. Med. Sci.* **68**, 1218–1225 (2013).
48. R. M. Zebaze *et al.*, Intracortical remodelling and porosity in the distal radius and post-mortem femurs of women: A cross-sectional study. *Lancet* **375**, 1729–1736 (2010).
49. X. He *et al.*, Sox9 positive periosteal cells in fracture repair of the adult mammalian long bone. *Bone* **103**, 12–19 (2017).
50. Y. Shi *et al.*, Gli1 identifies osteogenic progenitors for bone formation and fracture repair. *Nat. Commun.* **8**, 2043 (2017).
51. C. Mo *et al.*, Single-cell transcriptomics of LepR-positive skeletal cells reveals heterogeneous stress-dependent stem and progenitor pools. *EMBO J.* **41**, e108415 (2022).
52. B. Gao *et al.*, Macrophage-lineage TRAP+ cells recruit periosteum-derived cells for periosteal osteogenesis and regeneration. *J. Clin. Invest.* **129**, 2578–2594 (2019).
53. A. F. Schilling *et al.*, High bone mineral density in pycnodysostotic patients with a novel mutation in the propeptide of cathepsin K. *Osteoporos Int.* **18**, 659–669 (2007).
54. K. Soe, D. M. Merrild, J. M. Delaisse, Steering the osteoclast through the demineralization-collagenolysis balance. *Bone* **56**, 191–198 (2013).
55. G. Motyckova, D. E. Fisher, Pycnodysostosis: Role and regulation of cathepsin K in osteoclast function and human disease. *Curr. Mol. Med.* **2**, 407–421 (2002).
56. T. Cusick *et al.*, Odanacatib treatment increases hip bone mass and cortical thickness by preserving endocortical bone formation and stimulating periosteal bone formation in the ovariectomized adult rhesus monkey. *J. Bone Miner Res.* **27**, 524–537 (2012).
57. C. Jerome, M. Missbach, R. Gamse, Balicatib, a cathepsin K inhibitor, stimulates periosteal bone formation in monkeys. *Osteoporos Int* **23**, 339–349 (2012).
58. S. Lotinun *et al.*, Osteoclast-specific cathepsin K deletion stimulates S1P-dependent bone formation. *J. Clin. Invest.* **123**, 666–681 (2013).
59. B. L. Pennypacker *et al.*, Inhibition of cathepsin K increases modeling-based bone formation, and improves cortical dimension and strength in adult ovariectomized monkeys. *J. Bone Miner Res.* **29**, 1847–1858 (2014).
60. T. Duong, A. T. Leung, B. Langdahl, Cathepsin K inhibition: A new mechanism for the treatment of osteoporosis. *Calcif. Tissue Int.* **98**, 381–397 (2016).
61. K. Nakashima *et al.*, The novel zinc finger-containing transcription factor osterix is required for osteoblast differentiation and bone formation. *Cell* **108**, 17–29 (2002).
62. M. Tsukasaki *et al.*, Periosteal stem cells control growth plate stem cells during postnatal skeletal growth. *Nat. Commun.* **13**, 4166 (2022).
63. N. Bonnet, J. Brun, J. C. Rousseau, L. T. Duong, S. L. Ferrari, Cathepsin K controls cortical bone formation by degrading periostin. *J. Bone Miner Res.* **32**, 1432–1441 (2017).
64. I. S. Maggiano, C. M. Maggiano, V. G. Tiesler, J. R. Chi-Keb, S. D. Stout, Drifting diaphyses: Asymmetry in diametric growth and adaptation along the humeral and femoral length. *Anat Rec. (Hoboken)* **298**, 1689–1699 (2015).
65. S. Lotinun *et al.*, Cathepsin K-deficient osteocytes prevent lactation-induced bone loss and parathyroid hormone suppression. *J. Clin. Invest.* **129**, 3058–3071 (2019).
66. H. Qing *et al.*, Demonstration of osteocytic perilacunar/canalicular remodeling in mice during lactation. *J. Bone Miner Res.* **27**, 1018–1029 (2012).
67. B. Yu *et al.*, Wnt4 signaling prevents skeletal aging and inflammation by inhibiting nuclear factor-kappaB. *Nat. Med.* **20**, 1009–1017 (2014).
68. X. Li *et al.*, Type II collagen-positive progenitors are important stem cells in controlling skeletal development and vascular formation. *Bone Res.* **10**, 46 (2022).
69. P. T. Newton *et al.*, A radical switch in clonality reveals a stem cell niche in the epiphyseal growth plate. *Nature* **567**, 234–238 (2019).
70. N. Ono, W. Ono, T. Nagasawa, H. M. Kronenberg, A subset of chondrogenic cells provides early mesenchymal progenitors in growing bones. *Nat. Cell Biol.* **16**, 1157–1167 (2014).
71. N. Sakagami, W. Ono, N. Ono, Diverse contribution of Col2a1-expressing cells to the craniofacial skeletal cell lineages. *Orthod Craniofac Res.* **20**, 44–49 (2017).
72. M. A. Serowoky, C. E. Arata, J. G. Crump, F. V. Mariani, Skeletal stem cells: Insights into maintaining and regenerating the skeleton. *Development* **147**, dev179325 (2020).
73. P. Beighton, Pyle disease (metaphyseal dysplasia). *J. Med. Genet.* **24**, 321–324 (1987).
74. E. Pyle, A case of unusual bone development. *J. Bone Joint Surg Am.* **13**, 874–876 (1931).
75. W. L. Gadegone, V. Lokhande, Fracture femur in a case of Pyle's disease: A case report. *Surgical Sci.* **6**, 478–482 (2015).
76. S. K. Y. Gupta, A. B. Jayanth, Pyle's disease: A rare case report on 13 year female child. *J. Med. Case Rep. Case Series* **1** (2020), 10.38207/jmcrcs20201058.
77. B. Boward, T. Wu, S. Dalton, Concise review: Control of cell fate through cell cycle and pluripotency networks. *Stem. Cells* **34**, 1427–1436 (2016).
78. D. W. Hagey *et al.*, Distinct transcription factor complexes act on a permissive chromatin landscape to establish regionalized gene expression in CNS stem cells. *Genome Res.* **26**, 908–917 (2016).
79. J. Muhr, D. W. Hagey, The cell cycle and differentiation as integrated processes: Cyclins and CDKs reciprocally regulate Sox and Notch to balance stem cell maintenance. *Bioessays* **43**, e2000285 (2021).
80. B. Langdahl, S. Ferrari, D. W. Dempster, Bone modeling and remodeling: Potential as therapeutic targets for the treatment of osteoporosis. *Ther Adv. Musculoskelet Dis.* **8**, 225–235 (2016).
81. B. Z. Leder, Parathyroid hormone and parathyroid hormone-related protein analogs in osteoporosis therapy. *Curr. Osteoporos Rep.* **15**, 110–119 (2017).
82. B. C. Silva, J. P. Bilezikian, Parathyroid hormone: Anabolic and catabolic actions on the skeleton. *Curr. Opin. Pharmacol.* **22**, 41–50 (2015).
83. L. F. Bonewald, The amazing osteocyte. *J. Bone Miner. Res.* **26**, 229–238 (2011).
84. Y. Rhee *et al.*, PTH receptor signaling in osteocytes governs periosteal bone formation and intracortical remodeling. *J. Bone Miner Res.* **26**, 1035–1046 (2011).
85. M. N. Wein, H. M. Kronenberg, Regulation of bone remodeling by parathyroid hormone. *Cold Spring Harb. Perspect. Med.* **8**, a031237 (2018).
86. E. R. Moore, M. Feigenson, D. E. Maridas, Transverse fracture of the mouse femur with stabilizing pin. *J. Vis. Exp.* **178**, e63074 (2021), 10.3791/63074.
87. D. W. Dempster *et al.*, Standardized nomenclature, symbols, and units for bone histomorphometry: A 2012 update of the report of the ASBMR Histomorphometry Nomenclature Committee. *J. Bone Miner Res.* **28**, 2–17 (2013).
88. M. L. Bouxsein *et al.*, Guidelines for assessment of bone microstructure in rodents using micro-computed tomography. *J. Bone Miner Res.* **25**, 1468–1486 (2010).